PLOS PATHOGENS

Genome wide CRISPR screen for *Pasteurella multocida* toxin (PMT) binding proteins reveals LDL Receptor Related Protein 1 (LRP1) as crucial cellular receptor

Julian Schoellkopf[1], Thomas Mueller[1], Lena Hippchen[1], Teresa Mueller[2], Raphael Reuten[1], Rolf Backofen[2,3], Joachim Orth[1], Gudula Schmidt[1] *

1 Institute for Experimental and Clinical Pharmacology and Toxicology, Faculty of Medicine, Albert-Ludwigs-University, Freiburg, Germany, 2 Bioinformatics—Department of Computer Science, Albert-Ludwigs-University, Freiburg, Germany, 3 Signalling Research Centres BIOSS and CIBSS, Albert-Ludwigs-University, Freiburg, Germany

* Gudula.Schmidt@pharmakol.uni-freiburg.de

Abstract

PMT is a protein toxin produced by *Pasteurella multocida* serotypes A and D. As causative agent of atrophic rhinitis in swine, it leads to rapid degradation of the nasal turbinate bone. The toxin acts as a deamidase to modify a crucial glutamine in heterotrimeric G proteins, which results in constitutive activation of the G proteins and permanent stimulation of numerous downstream signaling pathways. Using a lentiviral based genome wide CRISPR knockout screen in combination with a lethal toxin chimera, consisting of full length inactive PMT and the catalytic domain of diphtheria toxin, we identified the LRP1 gene encoding the Low-Density Lipoprotein Receptor-related protein 1 as a critical host factor for PMT function. Loss of LRP1 reduced PMT binding and abolished the cellular response and deamidation of heterotrimeric G proteins, confirming LRP1 to be crucial for PMT uptake. Expression of LRP1 or cluster 4 of LRP1 restored intoxication of the knockout cells. In summary our data demonstrate LRP1 as crucial host entry factor for PMT intoxication by acting as its primary cell surface receptor.

Author summary

Pathogenic bacteria produce and release protein toxins which enter mammalian cells to dictate their appearance and behavior. Frequently, these toxins are enzymes which modify specific targets within the cells. Therefore, a lot of those proteins comprise everything needed for host cell binding and uptake into the cytosol. Such toxins are named AB toxins, because they encompass binding properties (B) and catalytic activity (A) in a single protein. *Pasteurella multocida*, a gram-negative bacterium mostly involved in zoonotic diseases produces the large (146 kDa) AB protein toxin Pasteurella multocida toxin (PMT) as major virulence factor. PMT is a deamidase which activates heterotrimeric G proteins. This leads to direct and permanent stimulation of numerous signaling pathways. Using a

knockout library, we identified the LDL Receptor Related Protein1 (LRP1, CD91) as a crucial cellular receptor for PMT binding and uptake. Knockout of LRP1 or competition with a specific ligand prohibits binding, uptake and intoxication of mammalian cells. More than 40 distinct ligands have been identified to interact with LRP1 including apolipoproteins and cholesteryl esters, viruses and bacterial toxins. Therefore, LRP1 may act as a common pharmacological target to interfere with uptake of disease-inducing molecules.

Introduction

Pasteurella multocida, a gram-negative bacterium mostly involved in zoonotic diseases like pasteurellosis and atrophic rhinitis, produces the large (146 kDa) AB protein toxin *Pasteurella multocida* toxin (PMT) as major virulence factor. PMT is a deamidase which modifies a specific glutamine in the switch-II region of the alpha subunits of heterotrimeric G proteins (G_i, G_q and $G_{12/13}$) [1]. This leads to direct and permanent activation and stimulation of numerous signaling pathways ending up in mitogenic signaling, reorganization of the cytoskeleton, de-differentiation and many other cellular responses [2]. In pigs, *Pasteurella multocida* causes atrophic rhinitis with severe degradation of the turbinate bone [3]. Therefore, in this zoonotic disease main target cells of PMT are osteoclasts, osteoblasts and osteocytes. The toxin stimulates osteoclastogenesis and inhibits osteoblast differentiation [4]. Moreover, osteocytes are activated to stimulate the differentiation of osteoclast precursor cells by increased secretion of the receptor activator of nuclear factor κB ligand (RANKL) [5]. In humans, pasteurellosis is mainly caused by bites or scratches by infected animals possibly leading to systemic infection and selection of different target cells.

Following binding to a cellular receptor, PMT is taken up into mammalian cells by receptor-mediated endocytosis. It is then released into the cytosol from acidified endosomes. In the presence of Bafilomycin A1, an inhibitor of the endosomal proton pump (blocking acidification), intoxication by PMT is completely abolished [6]. However, the exact mechanism how PMT crosses the endosomal membrane is not known. Like many protein toxins, PMT is composed of the typical functional domains of bacterial AB toxins. Receptor binding and translocation through the endosomal membrane is mediated by the N-terminal amino acids 1 to 575, which are sufficient for transport of protein cargos like GFP into cells [6]. The C-terminal domains C1 to C3 are not involved in cellular uptake but mediate the catalytic activity. The minimal region encompassing the deamidase activity (C3) is located at the very C-terminus of the toxin (residues 1106 to 1285) with the catalytic triad typically present in deamidases: Cys1165, His1205 and Asp1220. The C1 domain (residues 576 to720) mediates attachment to the inner surface of the cellular plasma-membrane, while the function of domain C2 (residues 721 to 1105) has not been elucidated (S1 Fig, for review see [7,8]).

Bacterial protein toxins need a cell surface molecule to interact with. This could be a sugar, a lipid, a protein or a combination of several surface molecules. Early analysis suggested gangliosides as cellular receptors for PMT [9], however more precise biochemical and cell biological studies suggested sphingomyelin and positively charged membrane lipids as binding partners for PMT [10]. Treatment of cells with either sphingomyelinase, phospholipase and also incubation of cells with the protease trypsin reduced binding of PMT to the cell surface. Therefore, a putative protein receptor as additional binding component for the toxin has been suggested [10].

In this study we established a CRISPR/Cas9 based knockout screen for identification of the cellular receptor for PMT mainly following the excellent work performed by the group of Y.

Horiguchi [11]. The method selects cells which are not killed by the toxin or the toxin chimera of interest because an essential protein for binding, uptake or modification of the target is missing due to gene knockout. However, PMT itself is not able to kill cells. Therefore, we generated a fusion toxin composed of the catalytically inactive mutant of PMT (PMT-C1165S) and the functional catalytic domain of *Corynebacterium diphtheriae* toxin (DTa) (PMT-DTa, S1 Fig) [12]. Diphtheria toxin catalyzes the ADP-ribosylation of elongation factor thermo unstable (EF-Tu) which leads to its inactivation and therefore to the block of protein synthesis and eventually cell death. Ribosylation occurs at a diphthamide, a post-translationally modified histidine in EF-Tu [13,14]. For an effective and target-oriented search for the cellular receptor, we generated the following knockout screen: A mouse embryonic fibroblast (MEF) cell line was generated which stably expresses FLAG-Cas9-EGFP [11]. These cells were transduced with a lentiviral CRISPR library targeting 18424 different genes across the mouse genome (Add Gene, Kosuke Yusa). We used a multiplicity of infection (MOI) of 0.3 to generate mainly single gene knockouts by avoiding multiple transduction. Cells were than treated with the PMT-DTa chimera. Non-transduced cells as well as cells with a functional receptor and uptake machinery are killed by the toxin. Only cells with a receptor knockout or cells which block the toxins activity (for example by defective endocytosis) survive treatment with the fusion toxin. These cells were further amplified and genomic DNA was extracted. Sequences which encode the single guide RNAs within the genome of the transduced cells correspond to the respective genes which are knocked out. These sequences were amplified and analyzed by next generation sequencing (Eurofins). A schematic overview of the method is shown in Fig 1.

Using this CRISPR knockout approach, we identified the LDL Receptor Related Protein1 (LRP1, CD91) as a cellular receptor crucial for PMT binding and uptake. LRP1 belongs to the family of low-density lipoprotein receptors. More than 40 distinct ligands have been identified to interact with LRP1 including apolipoproteins and cholesteryl esters in remnants [15,16], extracellular matrix (ECM) components such as fibronectin [17,18], a minor-group common cold virus [19] and Rift Valley fever virus [20] as well as bacterial toxins like *Clostridium perfringens* TpeL [21], *Pseudomonas* Exotoxin A (ExoA, [22]), TcdA produced by *Clostridoides difficile* [23] and the vacuolating toxin (VacA) from *Helicobacter pylori* [24]. These diverse ligands do not contain a common binding motif. Thus, LRP1 is suggested to be a general endocytosis receptor.

Results

Identification of essential binding partners for PMT on mammalian cells

We used a CRISPR/Cas9 based knockout screen for identification of the cellular receptor for the bacterial toxin *Pasteurella multocida* toxin (PMT). In this screen, only cells with a receptor knockout, cells with defective endocytosis or cells which block the toxins catalytic activity due to a missing protein should survive treatment with the fusion protein PMT-DTa. These cells were further amplified, genomic DNA extracted and sequences encoding the single guide RNA were analyzed by next generation sequencing (Eurofins). Significantly recovered sgRNAs and their corresponding genes were identified. The results are presented in Figs 2 and S2.

Two genes (Dph 1 und Dph 5) encoding enzymes required for diphthamide biosynthesis were present within the first ten hits. Diphthamide is a histidine which is post translationally modified in some proteins. Since diphtheria toxin selectively modifies a diphthamide present in elongation factor 2, the enzymes identified are crucial for the toxins action. Therefore, these targets demonstrate a reasonable readout of our CRISPR screen. The top hit in the screen and the only transmembrane cell surface protein was the Low-Density Lipoprotein Receptor-
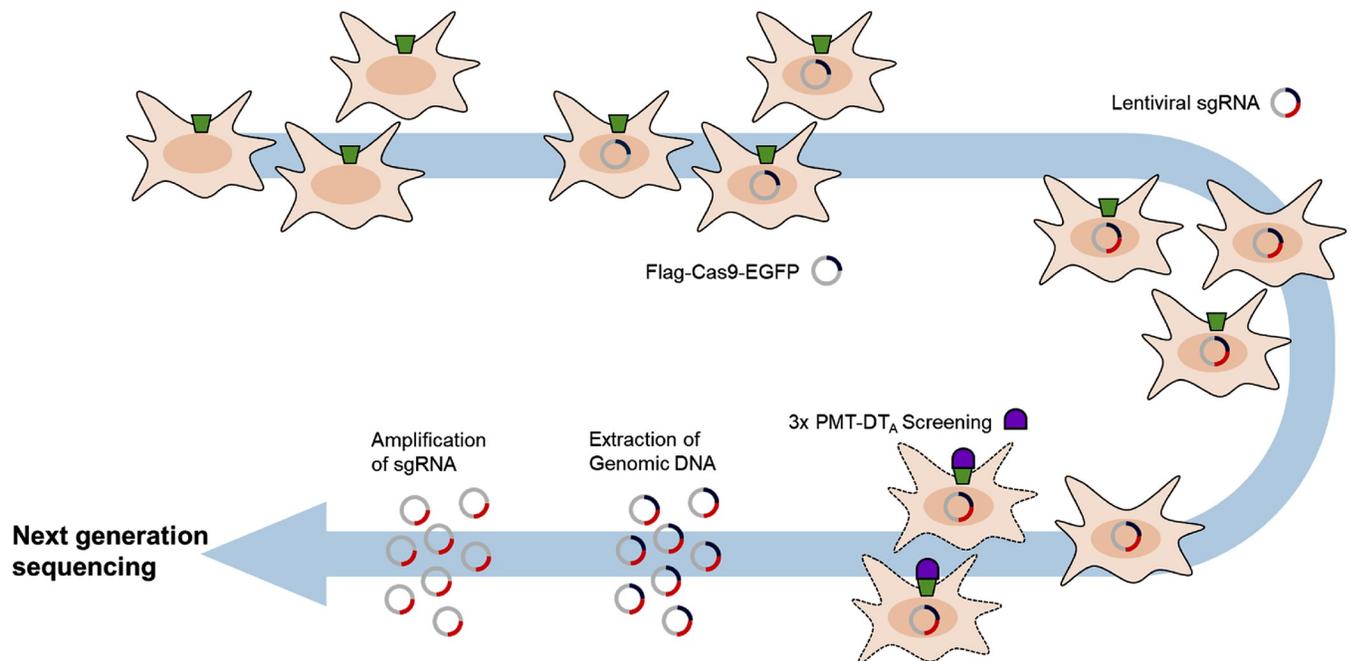
Fig 1. Schematic presentation of the CRISPR/Cas9-Knock out screen. Mouse embryonic fibroblasts (MEF) stably expressing Flag-Cas9-EGFP were transduced with a lentiviral CRISPR-library. Cells were treated three times with PMT(C1165S)DTa and surviving cells grown. Genomic DNA was extracted, inserted sgRNA amplified and sequenced.

https://doi.org/10.1371/journal.ppat.1010781.g001

related protein 1 (LRP1) (S2 Fig). LRP1 belongs to the family of low-density lipoprotein receptors and is highly expressed in many tissues, including the respiratory system (proteinatlas. org), an important entrance for *Pasteurella multocida*. The LRP1 protein is composed of four extracellular domains (cluster 1–4), a transmembrane and a cytoplasmic domain.

LRP1 knockout prohibits binding and uptake of PMT

To analyze whether LRP1 is crucial for binding and uptake of PMT, we used mouse embryonic fibroblasts (MEF) deficient for the LRP1 gene [25].

First, we studied viability of cells treated with the fusion toxin PMT-DTa in a concentration-dependent manner. In case LRP1 would be crucial for toxin binding and/or uptake, the knockout cells should survive. In Fig 3A cell viability was plotted in % of living wildtype fibroblasts and LRP1 knockout fibroblasts (LRP1$^{-/-}$) normalized to the respective untreated control with increasing concentration of PMT-DTa. Whereas the wildtype MEFs are killed already at low concentrations of PMT-DTa, there was no effect on the LRP1 knockout cells even at high concentrations. This indicates that LRP1 is crucial for binding/uptake of the fusion toxin. To study whether this holds true for PMT without DTa, we analyzed the binding properties of Alexa488 labeled PMT (PMT$_{488}$) to each cell line by FACS. As shown in Fig 3B, binding of PMT$_{488}$ to both cell lines increased in a concentration-dependent manner. However, fluorescence intensity of wildtype cells was much higher compared to LRP1$^{-/-}$ cells. Moreover, at higher concentrations of PMT$_{488}$ (0.5 to 1 μM) the binding curve seems to approach maximal values, indicating a saturable receptor on the cell surface. Our data suggest that LRP1 is involved in binding of PMT to mammalian cells. To study whether the binding of PMT$_{488}$ to LRP1 is crucial for intoxication, we directly studied PMT-induced intoxication of MEF wildtype and LRP1 knockout cells. Therefore, we made use of an antibody which detects
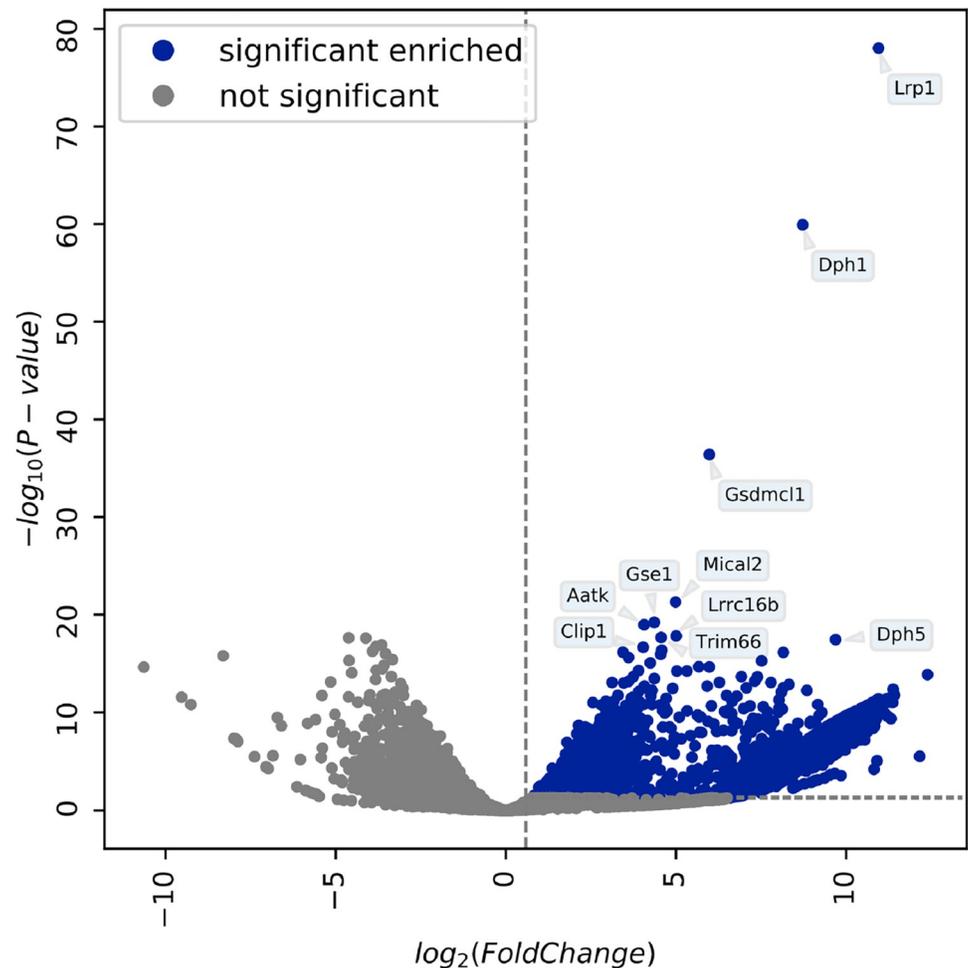
Fig 2. Volcano plot showing significantly enriched genes. The volcano plot shows gene expression changes between cells surviving treatment with usually lethal PMT-DTa chimera and those only transduced with the CRISPR library. All reads were mapped locally using BWA-MEM [5,6], then quantified with featureCounts [4], and finally fold changes between the condition were calculated by DESeq2 [7] (see galaxy history). The volcano plot was drawn with the bioinfokit toolkit [8]. Significantly enriched genes, having a positive fold change above 0.584 and a p-value lower or equal 5%, are shown in blue. The significance thresholds are marked by gray-dotted lines. The ten most significant genes are highlighted with their name. Non-significant genes are colored in gray.

https://doi.org/10.1371/journal.ppat.1010781.g002

deamidated Gα (Gα Q209E). Wildtype and knockout MEF were treated with PMT for 2 to 6 h or left untreated. Cells were lysed and the lysates analyzed for deamidated Gα, the presence of LRP1 and tubulin as loading control by Western-blotting as indicated. As shown in Fig 4 (top), the G proteins in the lysates of wildtype MEF were already deamidated 2 h following toxin treatment, whereas there was only minimal deamidation detectable in the lysates of LRP1$^{-/-}$ cells up to 6 h after PMT exposure. The data indicate that LRP1 is crucial for uptake of PMT into cells and thus for intoxication. The residual modification of G proteins in LRP1$^{-/-}$ cells may be due to unspecific toxin binding and uptake or due to binding to a protein which so far is unidentified or positively charged membrane lipids [10]. However, LRP1 seems to be crucial for an effective uptake of the toxin into mammalian cells. To further strengthen the finding, we made use of a known chaperone and ligand of LRP1, receptor-associated protein (RAP) to compete with PMT for LRP1 binding [26]. Therefore, MEF were incubated with buffer, 1 nM or 10 nM of PMT, respectively in the presence or absence of recombinant
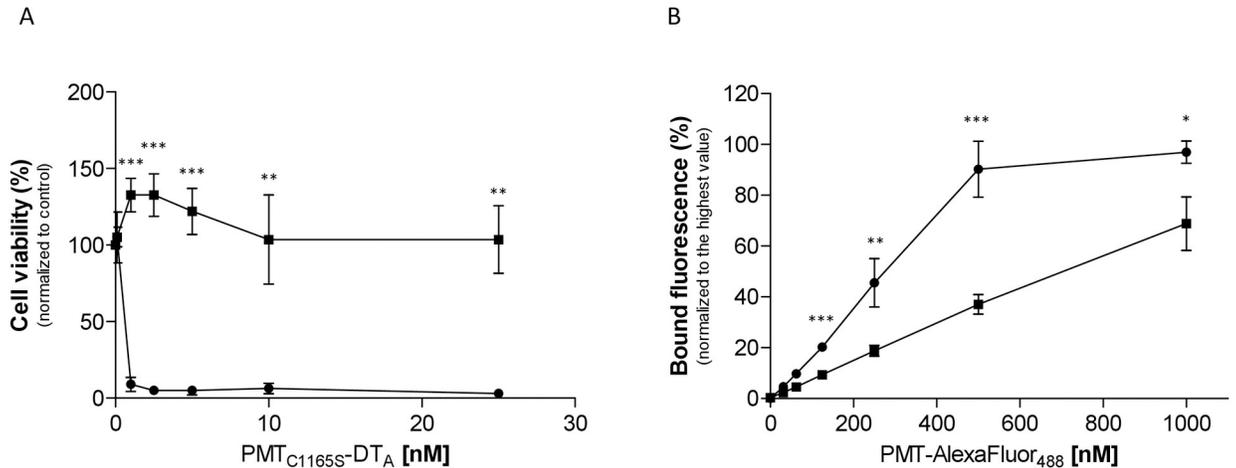
A

B

Fig 3. LRP1 knockout prohibits binding and uptake of PMT. MEF (circles) and MEF-LRP1$^{-/-}$ cells (squares), respectively were incubated with increasing concentrations of PMT(C1165S)DTa for 48h and cell viability was analyzed as % of untreated controls. Shown is the mean of three independent experiments (A). Cells were incubated with increasing concentrations of Alexa488 labeled PMT (PMT$_{488}$), washed and bound fluorescence analyzed by FACS shown as mean of three independent experiments (B).

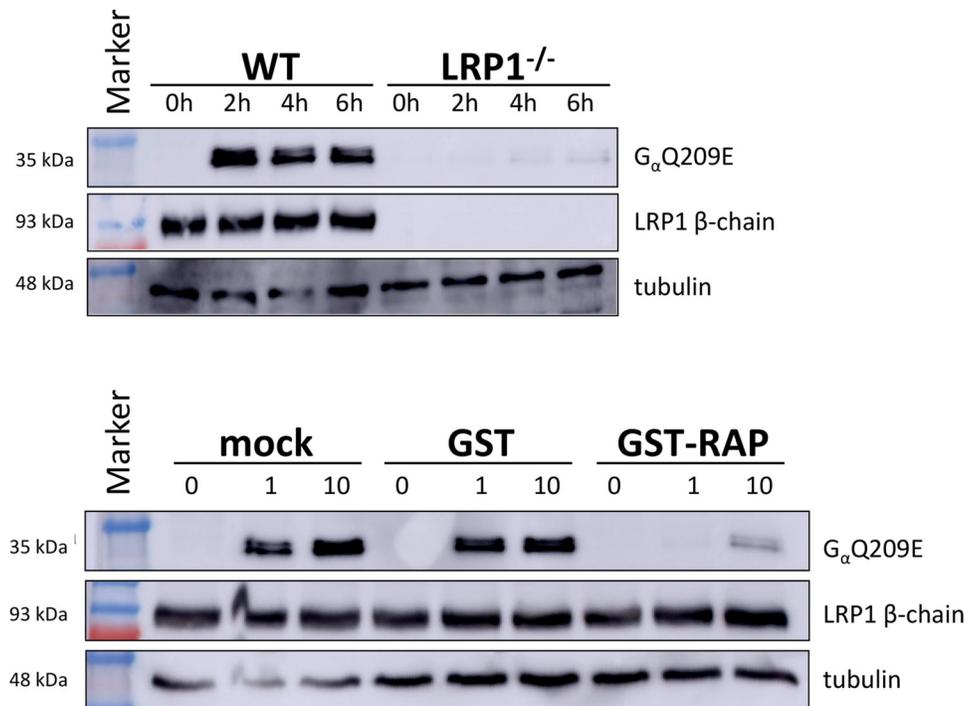https://doi.org/10.1371/journal.ppat.1010781.g003

Fig 4. LRP1 knockout or competitive inhibition of LRP1 inhibit modification of PMT. MEF and MEF-LRP1$^{-/-}$ cells were incubated in the presence of 5nM PMT for the indicated time intervals, washed and lysed. Lysates were analyzed for toxin-induced modification of Gαq by an antibody detecting GαQ209E, for expression of LRP1 and for tubulin as loading control (top). MEF and MEF-LRP1$^{-/-}$ cells were incubated in the presence of 1 or 10 nM PMT in the presence or absence of GST or GST-RAP (1 μM), respectively, washed and lysed. Lysates were analyzed for toxin-induced modification of Gαq, for expression of LRP1 and for tubulin as loading control (c, bottom). Statistics: [*], p < 0.05; [**], p < 0.01; [***], p < 0.001.

https://doi.org/10.1371/journal.ppat.1010781.g004

glutathione-S-transferase (GST) or GST-RAP (1 μM each), incubated for 2h, washed and lysed. Lysates were then analyzed for deamidated Gα. As shown in Fig 4 (bottom), deamidation of Gα in PMT-treated cells was significantly reduced when the cells were co-incubated with GST-RAP, but not in toxin-treated cells co-treated with GST. This indicates that GST-RAP but not GST interfered with the binding/action of PMT, suggesting a crucial role of the RAP receptor LRP1 for intoxication with PMT.

Direct interaction of LRP1 and PMT

To study a potential direct interaction between LRP1 and PMT, we performed a solid-phase binding assay with recombinantly produced PMT and the commercially available extracellular domains (cluster 2–4) of LRP1, respectively. These data reveal that while cluster 3 was dispensable for the PMT-LRP1 interaction PMT strongly bound to cluster 2 and 4, respectively (Fig 5). In our experiments, cluster 4 bound 18-fold stronger to PMT with a K_D of 2.278 nM in comparison to cluster 2 with a K_D of 41,65 nM.

Cluster 4 of LRP1 is sufficient for PMT binding

Affinities of recombinant proteins indicate that it is mainly cluster 2 and 4 of LRP1, respectively which mediate binding of PMT with the highest affinity measured between cluster 4 and the toxin. For most viruses and bacterial toxins which interact with LRP1, the membrane closest domain (cluster 4) has been shown to be sufficient for binding and endocytosis [21]. Therefore, we intended to rescue intoxication of LRP1$^{-/-}$ cells with full-length LRP1 and with cluster 4 of LRP1, respectively. To this end, we transfected the knockout cells with plasmids encoding for the respective proteins or with the empty vector and incubated them with PMT. Whereas
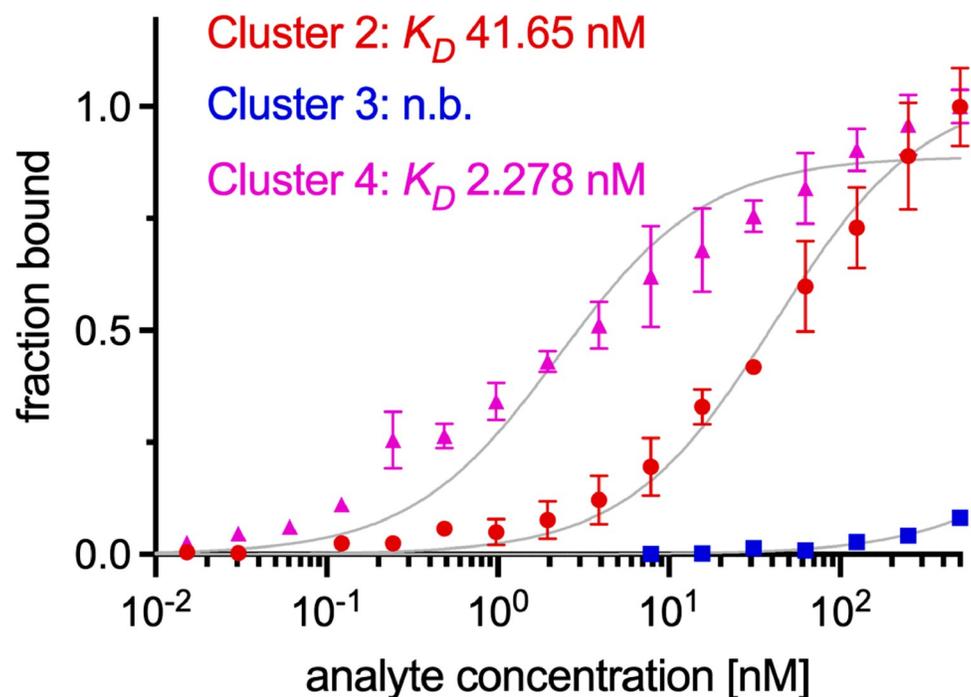

Fig 5. Solid-phase binding assay of PMT to clusters 2, 3, and 4 of LRP1. Graph depicts the binding curves of cluster 2 (dots), 3 (squares), and 4 (triangles) to plates coated with His-PMT. The equilibrium-binding affinity (K_D) is presented inside the graph. Data are shown as mean with STDEV.
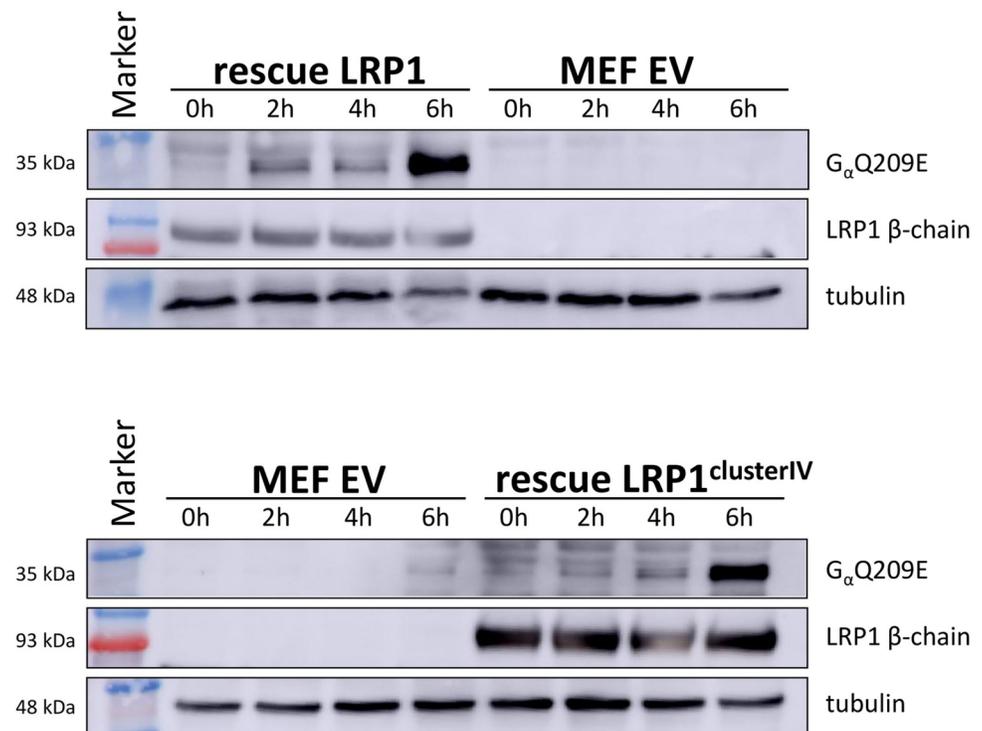
https://doi.org/10.1371/journal.ppat.1010781.g005

Fig 6. Expression of LRP1 or LRP1 cluster 4 in MEF-LRP1$^{-/-}$ cells restores the ability of PMT to intoxicate cells. MEF-LRP1$^{-/-}$ cells were transduced with retroviruses encoding LRP1 (top) or LRP1-cluster 4 (bottom), incubated in the presence of 5 nM PMT for the indicated time intervals, washed and lysed. Lysates were analyzed for toxin-induced modification of GαQ, for expression of LRP1 and for tubulin as loading control.

in cells transfected with the empty vector Gαq is not deamidated upon treatment with PMT, the protein is modified in cells re-expressing LRP1 with the maximal amount of deamidated Gαq following 6 h of treatment (Fig 6, top). Similar results are received when we re-expressed exclusively cluster 4 of LRP1 together with the transmembrane beta chain, to ensure that the protein is localized correctly in the plasma membrane. In cells expressing cluster 4 of LRP1, Gαq is deamidated upon treatment with PMT with the maximal amount of deamidated Gα after 6 h of treatment (Fig 6, bottom). The data show that ectopic expression of LRP1 cluster 4 restores intoxication of LRP1 knockout cells in the same manner as re-expression of LRP1 does and therefore suggest that cluster 4 sufficiently mediates binding and uptake of PMT.

Discussion

The aim of this study was to identify the cell surface receptor/s for the bacterial toxin PMT. The toxin is the main virulence factor of *Pasteurella multocida*. The non-motile, gram-negative bacterium causes diseases in animals like the atrophic rhinitis in swine. This disease is accompanied by destruction of the turbinate bone and general growth retardation [3,27]. Osteoblasts and osteoclasts seem to be main target cells of PMT. The toxin stimulates osteoclasts directly and on the other hand represses osteoblast differentiation [4]. Moreover, osteocytes are activated which stimulate the osteoclastogenesis by increased secretion of the receptor activator of nuclear factor κappa B ligand (RANKL) [5]).

Using the CRISPR screen established, we identified LRP1 as top hit of the genes which when knocked out block intoxication by the PMT-DTa chimera. In line with the role of LRP1 in PMT pathophysiology of atrophic rhinitis, LRP1 signaling itself has been suggested to be

involved in the differentiation of bone marrow derived macrophages into osteoclasts [28]. Moreover, LRP1 on the surface of osteoblasts regulates osteoblast-osteoclast interaction and RANKL signaling [29]. Both LRP1 functions may support toxin induced bone degradation. However, PMT induced LRP1 signaling has not been analyzed so far.

Pasteurella multocida is also found in oral secretions of dogs and cats and can cause wound infections, abscesses and osteomyelitis in man following animal bites. In immuno-compromised humans also respiratory infections with pneumonia have been described [30]. In fact, LRP1 is expressed in many tissues with the highest score in the respiratory system. LRP1 is encompassed of a single pass transmembrane protein composed of four extracellular domains (called cluster 1–4, LRP1α, 515 kDa) as well as a transmembrane and a cytoplasmic domain, which together form LRP1β (85 kDa). The two LRP parts originate from a single precursor-protein which is cleaved by furin within the endoplasmic reticulum [25]. The chaperone receptor associated protein (RAP) escorts LRP1 from the endoplasmic reticulum to the Golgi apparatus. The tight binding of RAP to LRP1 has been used for competition experiments proving newly identified receptor ligands [21]. On the cell surface the two parts remain non-covalently linked.

A variety of ligands have been shown to interact with LRP1 including apolipoproteins, viruses and bacterial toxins with no common binding motif identified in all these ligands.

Thus, LRP1 is regarded as general endocytosis receptor and moreover, LRP1 mediates intracellular signaling [31]. The receptor associated protein (RAP) acts as a chaperone during synthesis of LRP1 [32] and binds to the cell surface protein when added to culture medium. Therefore, the protein acts as a competitive inhibitor for ligands binding to LRP1 [21,26]. Moreover, RAP has been used to affinity-purify LRP1 from tissues [33]. In our experiments RAP competes with PMT for binding to LRP1 on cells. Since ligands for LRP1 include intracellular proteins like the nuclear protein high mobility group protein B1 (HMGB1) which is passively released upon injury, it was suggested that LRP1 has the additional function to remove such debris promoting wound healing [33]. Moreover, LRP1 seems to be involved in transcytosis and may mediate uptake of bacterial toxins and viruses through the epithelium into several deeper tissues. Our results do not exclude the possibility of transcytosis since a portion of the toxin which is endocytosed for transport through the cells may reach the cytosol and therefore would be able to deamidate Gα. Binding kinetics using a solid-phase binding assay analyzing the interaction between PMT and cluster 2, 3, and 4, respectively revealed that the toxin strongly binds to cluster 2 (K_D 41,65 nM) and 4 (K_D 2.278 nM), while cluster 3 is not required for PMT binding. The affinity of the interaction between cluster 4 of LRP1 with recombinant PMT is comparable to TpeL (KD: ~23,2 nM) and Pseudomonas exotoxin A (KD: ~5,2 nM) [21]. The data are in line with cluster 4 presenting the site most frequently identified as interaction surface between LRP1 and diverse ligands. Moreover, cluster 4 is sufficient to bind and take up PMT into mammalian cells. Cluster 4 representing the main binding partner for cargos is a little unexpected nevertheless, because it is the one located proximate to the plasma membrane.

Receptor expression is not the only factor which determines the efficiency of intoxication. Differences between cellular binding, uptake and translocation into the cytosol might be equally important: The general capacity of endocytosis, the velocity of acidification of the endosome, the amount of a potential second protein needed for induction of endocytosis, a different lipid composition or a specific lipid component of the membrane allowing binding and endocytosis of the LRP1-PMT complex. We compared HeLa cells which are less efficiently intoxicated by PMT with the more susceptible HepG2 (liver) cells. Therefore, we treated the cells with decreasing concentrations of PMT for 2 h, lysed the cells and studied modification of G proteins as well as the amounts of LRP1 and GAPDH, respectively by Western-blotting. Surprisingly, HeLa cells expressed nearly as much LRP1 (compared to GAPDH) as HepG1 cells

and bound similar amounts of labeled PMT in FACS experiments. However, they showed much lower modification of G proteins at an early time point (2h) which is equalized following overnight treatment with PMT (S3 Fig). These data show that expression of a protein receptor is necessary for intoxication but is not the exclusive determinant for its efficiency. Besides LRP1, two genes (Dph 1 and Dph 5) encoding enzymes required for diphthamide biosynthesis were present within the first ten hits of our screen. Diphtheria toxin selectively modifies a specific diphthamide of elongation factor 2. The absence of diphthamide therefore blocks modification of EF2 and survival, proving the reasonable readout of our CRISPR screen. As control we used CAS9 expressing cells transduced with the CRISPR library but not treated with the toxin chimera. Therefore, the cells were collected earlier to use the same cell number for amplification of inserted sequences. Due to the cultivation time differences, we also expected enrichment of genes which influence proliferation. However, probably due to the strong selection force of the deadly toxin chimera, such genes were not found to be significantly enriched or diminished. In contrast, loss of tubulin binding proteins like Mical2 and Clip1 may be involved in endocytosis of PMT-DTa. Our screen may have missed further surface molecules which additionally may be important for PMT binding and/or uptake. Some genes knocked out may be essential for survival and would not be detected, others may not be presented within the library or casually lost during transduction. However, our data show that PMT binding and endocytosis is mediated by LRP1. Therefore, LRP1 may act as a common pharmacological target to interfere with uptake of disease-inducing viruses and bacterial toxins.

Materials and methods

Unmodified DNA oligonucleotides were obtained from biomers.net GmbH, while HPLC grade oligonucleotides from Eurofins Genomics were used for next generation sequencing. All other reagents were of analytical grade and purchased from different commercial sources.

Cell culture, media and growth conditions

HEK293T, HepG2 and Swiss3T3 cells were originally obtained from ATCC. MEF and MEF LRP1-/- were kindly provided by J. Herz (UT Southwestern, Dallas) and were already used in previous work of the lab. MEF EV, MEF LRP1-/-, MEF Rescue FL and MEF Rescue C4 were generated for previous work by B. Schorch (Universitätsklinikum Freiburg, Germany) and were already present at the lab. Cells were cultured in Dulbecco's modified Eagle's medium (DMEM) supplemented with 10% FCS, 1% P/S and 1% NEAA. The atmosphere of 5% CO_2 at 37°C was kept constantly in appropriate incubators.

Cell lysis

For generating lysates cells were treated with RIPA buffer (1 mM EDTA, 25 mM Tris, 150 mM NaCl, 1% (v/v) Triton X-100, pH 7.4), containing "Complete" protease inhibitor cocktail (Roche) for 15 min on ice with occasional mixing. Lysates were then centrifuged at 4°C (10,000 rpm for 10 min).

Cloning, Mutagenesis and purification of recombinant PMT and PMT(C1165S)DTa

PMT and PMT(C1165S)DTa were expressed as N-terminal His6-tagged proteins and purified by affinity chromatography via a Ni-NTA column as described previously [35].

Cas9-expressing MEF and Swiss3T3 cells

For generation of stable cell lines expressing Cas9 the piggyBac-transposon-transposase system was used. The plasmids carrying the transposase and the transposon (pCMV-hyPBase and

pPB-pgkNeo-CBh-hSpCas9n-EGFP) were gained and generated by Y. Horiguchi (Research institute of microbial diseases, Osaka). Cells were transfected by using Lipofectamine 2000 transfection reagent according to the manufacturer's instructions with subsequent antibiotic selection with G418. Surviving cells were isolated via limiting dilution method to obtain independent clones. The clone with the highest GFP-signal was identified by using fluorescence microscopy and was further used as monoclonal origin of MEF-Cas9nEGFP and Swiss3T3-Cas9nEGFP.

Genome-wide CRISPR/Cas9-Knock out library and screening

Generation of genome-wide Cas9-sgRNA library and subsequent screening were performed as described by Teruya and adapted [11]. We utilized a well-functioning and validate genome-wide mouse lentiviral CRISPR guide RNA library v2 (Addgene). It consists of 90230 gRNA sequences directed against 18424 different genes across the mouse genome. HEK293T cells were co-transfected with library plasmids and suitable packaging- and envelope plasmids (CRISPR & MISSION Lentiviral packaging mix, Sigma-Aldrich) by using Lipofectamine 2000 Transfection Reagent according to the manufacturer's instructions. Lentiviral particles were obtained after 48 h via centrifugation of the culture supernatant at $1500 \times g$ for 15 min at 4°C and subsequent sterile filtration trough 0,45µm pore filters. The virus titer was quantified by an ELISA assay against the lentiviral envelope protein p24 (HIV1 p24 ELISA Kit, Abcam). The Cas9 expressing MEF cells were infected in presence of 8 µg/ml Polybrene with the lentiviral particles at a multiplicity of infection of 0,3 to avoid multiple gene knock outs in one cell. Following the infected cells were identified by antibiotic selection procedure by using 8 µg/ml Puromycin after 48 h.

For screening the library cells were incubated 3 times with 2µg/ml PMT-DTa for 36 h with an intermediate interval of 24 h in toxin-free full medium. The surviving cells were cultivated to confluence of a 6 well and the genomic DNA was isolated by incubation of the harvested cells with proteinase K at 37°C in accordance to instructions. The sgRNA containing sequences of the genomic template DNA were amplified by PCR using the indicated Primers of HPLC grade (Table 1) and Q5 Hot Start high-fidelity DNA polymerase (New England BioLabs). The PCR products of the toxin resistant cells and untreated library cells were analyzed by deep sequencing using an Illumina-based procedure via a commercial supplier (Eurofins Genomics).

Cell viability assay

The metabolic activity of MEF and MEF LRP1-/- cells (cell viability) was determined by using the CellTiter-Blue cell viability assay (Promega) following the manufacturer's protocol. The fluorescent product resofurin was measured on a multimode microplate reader (Infinite M200; Tecan).

Immunoblotting

For immunoblotting cell lysates were subjected to SDS-PAGE and electro transferred onto a PVDF membrane. After subsequent blocking and washing, PMT action was detected by a

Table 1. Oligonucelotides used in this study.

Oligonucleotide	Sequence
pST-Cas9-S27 #sample1	AGTCATTGAGCTTGAAAGTATTTCGATTTCTTGG
pST-Cas9-S27 #sample2	GATCTCATTCCTTGAAAGTATTTCGATTTCTTGG
pST-Cas9-S27 #sample3	CGCTTATCCTCTTGAAAGTATTTCGATTTCTTGG
pST-Cas9-AS28	ACTCGGTGCCACTTTTTCAA

Table 2. Antibodies used in this study.

Antibody	Source
GαQ209E	self-produced in hybridoma cells [34]
LRP1	Abcam
Tubulin	Santa Cruz
GAPDH	Santa Cruz
Anti-rat IgG HRP	Cell Signaling
Anti-goat IgG HRP	Cell Signaling
Anti-mouse IgG HRP	Rockland Inc.

https://doi.org/10.1371/journal.ppat.1010781.t002

deamidation specific antibody anti-GαqQ209E as described before [34]. LRP1 and tubulin were visualized by suitable antibodies given in Table 2. By utilizing SignalFire enhanced chemiluminescent detection reagent (Cell Signaling Technology) and the imaging system LAS-3000 (Fujifilm), binding of the compatible horseradish peroxidase-coupled secondary antibody was detected.

Solid-phase binding assay

N-terminally His-tagged *Pasteurella multocida* toxin (PMT) was coated at 10 μg/mL (500 ng/well) onto 96-well plates (NuncMaxisorb) at 4˚C overnight. After washing three times with TBS supplemented 2 mM $CaCl_2$, plates were blocked with Pierce™ protein-free TBS blocking solution (pH 7.4; Thermo Fisher Scientific) at room temperature (RT) for 2 h. Ligands (LRP1 cluster 2, 3, and 4) were diluted to concentrations from 0.02 nM to 500 nM and incubated at RT for 2 h. After extensive washing with TBS supplemented 2 mM $CaCl_2$, bound ligands were detected using a goat anti-human IgG-HRP-conjugated antibody (Santa Cruz, sc-2453; 1:4000). HRP was detected by Pierce TMB ELISA Substrate (Thermo Fisher Scientific). Absorption was measured at 450 nm after stopping the reaction with 2 M sulfuric acid. A blank value corresponding to BSA blocked wells of the respective analyte concentration was automatically subtracted.

FACS analysis

For binding studies PMT was labelled covalently with DyLight488 maleimide (Thermo Fisher Scientific) according to the manufacturer's instructions. Pre-cultured HeLa, HepG2 or MEF cells and derivates were detached from culture plates using 10 mM EDTA in PBS. For each condition 2×105–2.5×105 cells were used and incubated for 20 min with the indicated PMT-DyLight488 concentrations at 4˚C. Following several washing steps with ice-cold TBS, cell bound fluorescence was measured using a FACS Melody (BD Bioscience). Via the appropriate Software FACSChorus (BD Bioscience) 10.000 cells were analyzed. After gating and the average of surface bound fluorescence of all cells was given.

For analysis of surface bound fluorescence of cells, the median forward scatter of the analyzed Hela and HepG2 cell populations was measured for normalization.

Statistics

Statistical analysis and presentation were performed using the software GraphPadPrism 5 (GraphPad, San Diego, USA). Unless otherwise indicated, the mean value and the standard deviation the mean value and the calculated standard deviation (SD) are shown in all diagrams, unless otherwise stated, SD), are shown. P-values smaller than 0.5 were defined as

statistically significant and marked with an asterisk (n.s. = not significant; *, p < 0.05; **, p < 0.01; ***, p < 0.001; ****, p < 0.0001).

CRISPR data analysis

The gene expression changes analysis was performed using the three treated and two control single-end sequencing libraries. The sequencing quality was assessed using FastQC and MuliQC [36,37]. All read libraries were mapped against an sgRNA FASTA file, containing the full sgRNA library sequences, using BWA-MEM with an adjusted minimum score output of 18 and enabling penalties for 5'-end and 3'-end clipping [38,39]. Mapping rates were analyses using Samtools stats [40], resulting in an average rate 65%. The quantification was done using featureCounts [41]. The expression changes between the two conditions were calculated with DESeq2 [42]. The gene expression changes were summarized in a volcano plot using p-value 0.05 and LogFC 0.584 thresholds [43]. The full data analysis was performed in Galaxy, see: https://usegalaxy.eu/u/teresa-m/h/crisprsgrnadgeanalysis

Supporting information

S1 Fig. Schematic presentation of the toxins used. A: The *Pasteurella multocida* toxin (PMT) is composed of 5 domains: R: receptor binding domain, T: translocation domain containing two hydrophobic helices which are necessary for insertion into the endosomal membrane, C1-3: catalytic domain. C3 encodes for the deamidase domain. Mutation of C1165 to serine leads to a catalytically inactive toxin. B: Diphtheria toxin (DT) is composed of three domains: DTa is the catalytic domain, T: translocation domain, R: receptor binding domain. C: The fusion protein PMT(C1165S)DT$_a$ is composed of the catalytic inactive mutant of PMT and a c-terminally added catalytic domain of diphtheria toxin (DTa).
(PDF)

S2 Fig. Table depicting the 10 mostly enriched sgRNAs and the function of the targeted genes.
(PDF)

S3 Fig. Expression levels of LRP1 do not exclusively determine the efficiency of intoxication. HeLa and HepG2 cells were treated with the indicated concentrations of PMT for 2 h, or with 100 nM PMT for 16h as indicated, washed and lysed. A: Lysates were analyzed for toxin-induced modification of GαQ, LRP1 and GAPDH by Western-blotting. Shown is an example of 4 independent experiments. B: Quantification of the amount of LRP1 normalized to GAPDH in HeLa and HepG1 cells. C: HeLa and HepG2 cells were incubated with 1 μM Alexa 488 labeled PMT and washed. Cell bound fluorescence was analyzed by FACS in three independent experiments. Autofluorescence and relative cell size were used for normalizing bound fluorescence. Statistics: n.s: not significant, *, p < 0.05
(PDF)

Acknowledgments

Author Contributions

Conceptualization: Julian Schoellkopf, Thomas Mueller, Gudula Schmidt.

Data curation: Julian Schoellkopf, Thomas Mueller, Lena Hippchen, Teresa Mueller, Raphael Reuten, Gudula Schmidt.

Formal analysis: Teresa Mueller.

Funding acquisition: Rolf Backofen, Gudula Schmidt.

Investigation: Julian Schoellkopf, Thomas Mueller, Lena Hippchen.

Project administration: Joachim Orth.

Validation: Teresa Mueller.

Writing – original draft: Gudula Schmidt.

Writing – review & editing: Gudula Schmidt.

References

1. Orth JH, Aktories K. Pasteurella multocida toxin activates various heterotrimeric G proteins by deamidation. Toxins (Basel). 2010; 2(2):205–14. https://doi.org/10.3390/toxins2020205 PMID: 22069582

2. Orth JH, Lang S, Taniguchi M, Aktories K. Pasteurella multocida toxin-induced activation of RhoA is mediated via two families of G{alpha} proteins, G{alpha}q and G{alpha}12/13. J Biol Chem. 2005; 280 (44):36701–7. https://doi.org/10.1074/jbc.M507203200 PMID: 16141214

3. Lax AJ, Pullinger GD, Baldwin MR, Harmey D, Grigoriadis AE, Lakey JH. The pasteurella multocida toxin interacts with signalling pathways to perturb cell growth and differentiation. Int J Med Microbiol. 2004; 293(7–8):505–12. https://doi.org/10.1078/1438-4221-00287 PMID: 15149025

4. Strack J, Heni H, Gilsbach R, Hein L, Aktories K, Orth JH. Noncanonical G-protein-dependent modulation of osteoclast differentiation and bone resorption mediated by Pasteurella multocida toxin. MBio. 2014; 5(6):e02190. https://doi.org/10.1128/mBio.02190-14 [pii]; PMID: 25389180

5. Heni H, Ebner JK, Schmidt G, Aktories K, Orth JHC. Involvement of Osteocytes in the Action of Pasteurella multocida Toxin. Toxins (Basel). 2018; 10(8). Epub 2018/08/15. https://doi.org/10.3390/toxins10080328 PMID: 30104531; PubMed Central PMCID: PMC6115833.

6. Repella TL, Ho M, Chong TPM, Bannai Y, Wilson BA. Arf6-Dependent Intracellular Trafficking of Pasteurella multocida Toxin and pH-Dependent Translocation from Late Endosomes. Toxins. 2011; 3 (3):218–41. https://doi.org/10.3390/toxins3030218 PMID: 22053287

7. Wilson BA, Ho M. Pasteurella multocida: from Zoonosis to Cellular Microbiology. Clin Microbiol Rev. 2013; 26(3):631–55. https://doi.org/10.1128/CMR.00024-13 [pii]; PMID: 23824375

8. Wilson BA, Ho M. Pasteurella multocida Toxin Interaction with Host Cells: Entry and Cellular Effects. Curr Top Microbiol Immunol. 2012; 361:93–111. https://doi.org/10.1007/82_2012_219 PMID: 22552700

9. Pettit RK, Ackermann MR, Rimler RB. Receptor-mediated binding of Pasteurella multocida dermonecrotic toxin to canine osteosarcoma and monkey kidney (vero) cells. Lab Invest. 1993; 69(1):94–100. PMID: 8392646

10. Brothers MC, Ho M, Maharjan R, Clemons NC, Bannai Y, Waites MA, et al. Membrane interaction of Pasteurella multocida toxin involves sphingomyelin. FEBS J. 2011. https://doi.org/10.1111/j.1742-4658.2011.08365.x PMID: 21951695

11. Teruya S, Hiramatsu Y, Nakamura K, Fukui-Miyazaki A, Tsukamoto K, Shinoda N, et al. Bordetella Dermonecrotic Toxin Is a Neurotropic Virulence Factor That Uses CaV3.1 as the Cell Surface Receptor. mBio. 2020; 11(2). Epub 20200324. https://doi.org/10.1128/mBio.03146-19 PMID: 32209694; PubMed Central PMCID: PMC7157530.

12. Bergmann S, Jehle D, Schwan C, Orth JH, Aktories K. Pasteurella multocida toxin as a transporter of non-cell permeable proteins. Infect Immun. 2013; 81(7):2459–67. https://doi.org/IAI.00429-13 [pii]; PMID: 23630953

13. Evans DA, Lundy KM. Synthesis of diphthamide: The target of diphtheria toxin catalyzed ADP-ribosylation in protein synthesis elongation factor 2. J Am Chem Soc. 1992; 114:1495–6.

14. Liu S, Bachran C, Gupta P, Miller-Randolph S, Wang H, Crown D, et al. Diphthamide modification on eukaryotic elongation factor 2 is needed to assure fidelity of mRNA translation and mouse development. Proc Natl Acad Sci U S A. 2012; 109(34):13817–22. https://doi.org/10.1073/pnas.1206933109 PMID: 22869748; PubMed Central PMCID: PMC3427129.

15. Willnow TE, Goldstein JL, Orth K, Brown MS, Herz J. Low density lipoprotein receptor-related protein and gp330 bind similar ligands, including plasminogen activator-inhibitor complexes and lactoferrin, an inhibitor of chylomicron remnant clearance. J Biol Chem. 1992; 267(36):26172–80. PMID: 1464627

16. Kowal RC, Herz J, Goldstein JL, Esser V, Brown MS. Low density lipoprotein receptor-related protein mediates uptake of cholesteryl esters derived from apoprotein E-enriched lipoproteins. Proc Natl Acad Sci U S A. 1989; 86(15):5810–4. https://doi.org/10.1073/pnas.86.15.5810 PMID: 2762297

17. Lillis AP, Van Duyn LB, Murphy-Ullrich JE, Strickland DK. LDL receptor-related protein 1: unique tissue-specific functions revealed by selective gene knockout studies. Physiol Rev. 2008; 88(3):887–918. https://doi.org/10.1152/physrev.00033.2007 [pii] PMID: 18626063

18. Lillis AP, Greenlee MC, Mikhailenko I, Pizzo SV, Tenner AJ, Strickland DK, et al. Murine low-density lipoprotein receptor-related protein 1 (LRP) is required for phagocytosis of targets bearing LRP ligands but is not required for C1q-triggered enhancement of phagocytosis. J Immunol. 2008; 181(1):364–73. https://doi.org/10.4049/jimmunol.181.1.364 [pii]. PMID: 18566402

19. Hofer F, Gruenberger M, Kowalski H, Machat H, Huettinger M, Kuechler E, et al. Members of the low density lipoprotein receptor family mediate cell entry of a minor-group common cold virus. Proc Natl Acad Sci U S A. 1994; 91(5):1839–42. https://doi.org/10.1073/pnas.91.5.1839 PMID: 8127891

20. Ganaie SS, Schwarz MM, McMillen CM, Price DA, Feng AX, Albe JR, et al. Lrp1 is a host entry factor for Rift Valley fever virus. Cell. 2021; 184(20):5163–78 e24. Epub 20210923. https://doi.org/10.1016/j.cell.2021.09.001 PMID: 34559985; PubMed Central PMCID: PMC8786218.

21. Schorch B, Song S, van Diemen FR, Bock HH, May P, Herz J, et al. LRP1 is a receptor for Clostridium perfringens TpeL toxin indicating a two-receptor model of clostridial glycosylating toxins. Proc Natl Acad Sci U S A. 2014; 111(17):6431–6. https://doi.org/10.1073/pnas.1323790111 [pii]; PMID: 24737893

22. Pastrana DV, Hanson AJ, Knisely J, Bu G, FitzGerald DJ. LRP 1 B functions as a receptor for Pseudomonas exotoxin. Biochim Biophys Acta. 2005; 1741(3):234–9. https://doi.org/10.1016/j.bbadis.2005.06.007 [pii]; PMID: 16095885

23. Schottelndreier D, Langejurgen A, Lindner R, Genth H. Low Density Lipoprotein Receptor-Related Protein-1 (LRP1) Is Involved in the Uptake of Clostridioides difficile Toxin A and Serves as an Internalizing Receptor. Front Cell Infect Microbiol. 2020; 10:565465. Epub 20201019. https://doi.org/10.3389/fcimb.2020.565465 PMID: 33194803; PubMed Central PMCID: PMC7604483.

24. Nakayama M, Hisatsune J, Yamasaki E, Nishi Y, Wada A, Kurazono H, et al. Clustering of Helicobacter pylori VacA in lipid rafts, mediated by its receptor, receptor-like protein tyrosine phosphatase beta, is required for intoxication in AZ-521 Cells. Infect Immun. 2006; 74(12):6571–80. https://doi.org/10.1128/IAI.00356-06 PMID: 17030583; PubMed Central PMCID: PMC1698068.

25. Zurhove K, Nakajima C, Herz J, Bock HH, May P. Gamma-secretase limits the inflammatory response through the processing of LRP1. Sci Signal. 2008; 1(47):ra15. https://doi.org/10.1126/scisignal.1164263 [pii]; PMID: 19036715

26. Martin H, Willey B, Low DE, Staempfli HR, McGeer A, Boerlin P, et al. Characterization of Clostridium difficile Strains Isolated from Patients in Ontario, Canada, from 2004 to 2006. J Clin Microbiol. 2008; 46 (9):2999–3004. https://doi.org/10.1128/JCM.02437-07 PMID: 18650360

27. Lax A. The Pasteurella multocida Toxin: A New Paradigm for the Link Between Bacterial Infection and Cancer. Curr Top Microbiol Immunol. 2012; 361:131–44. https://doi.org/10.1007/82_2012_236 PMID: 22695919

28. Kohara Y, Haraguchi R, Kitazawa R, Kitazawa S. Knockdown of Lrp1 in RAW264 cells inhibits osteoclast differentiation and osteoclast-osteoblast interactions in vitro. Biochem Biophys Res Commun. 2020; 523(4):961–5. Epub 20200119. https://doi.org/10.1016/j.bbrc.2020.01.065 PMID: 31964526.

29. Bartelt A, Behler-Janbeck F, Beil FT, Koehne T, Muller B, Schmidt T, et al. Lrp1 in osteoblasts controls osteoclast activity and protects against osteoporosis by limiting PDGF-RANKL signaling. Bone Res. 2018; 6:4. Epub 20180226. https://doi.org/10.1038/s41413-017-0006-3 PMID: 29507818; PubMed Central PMCID: PMC5826921.

30. Mogilner L, Katz C. Pasteurella multocida. Pediatr Rev. 2019; 40(2):90–2. https://doi.org/10.1542/pir.2017-0178 PMID: 30709978.

31. Reekmans SM, Pflanzner T, Gordts PL, Isbert S, Zimmermann P, Annaert W, et al. Inactivation of the proximal NPXY motif impairs early steps in LRP1 biosynthesis. Cell Mol Life Sci. 2010; 67(1):135–45. Epub 20091025. https://doi.org/10.1007/s00018-009-0171-7 PMID: 19856143.

32. Willnow TE, Rohlmann A, Horton J, Otani H, Braun JR, Hammer RE, et al. RAP, a specialized chaperone, prevents ligand-induced ER retention and degradation of LDL receptor-related endocytic receptors. EMBO J. 1996; 15(11):2632–9. PMID: 8654360

33. Mogensen EH, Poulsen ET, Thogersen IB, Yamamoto K, Bruel A, Enghild JJ. The low-density lipoprotein receptor-related protein 1 (LRP1) interactome in the human cornea. Exp Eye Res. 2022; 219:109081. Epub 20220421. https://doi.org/10.1016/j.exer.2022.109081 PMID: 35461874.

34. Kamitani S, Ao S, Toshima H, Tachibana T, Hashimoto M, Kitadokoro K, et al. Enzymatic actions of Pasteurella multocida toxin detected by monoclonal antibodies recognizing the deamidated alpha subunit of the heterotrimeric GTPase G(q). FEBS J. 2011; 278(15):2702–12. https://doi.org/10.1111/j.1742-4658.2011.08197.x PMID: 21624053

35. Busch C, Orth J, Djouder N, Aktories K. Biological activity of a C-terminal fragment of *Pasteurella multocida* toxin. Infect Immun. 2001; 69:3628–34. https://doi.org/10.1128/IAI.69.6.3628-3634.2001 PMID: 11349023

36. Andrews S. FastQC: A Quality Control tool for High Throughput Sequence Data. Babraham Bioinformatics; 2010.

37. Ewels P, Magnusson M, Lundin S, Kaller M. MultiQC: summarize analysis results for multiple tools and samples in a single report. Bioinformatics. 2016; 32(19):3047–8. Epub 20160616. https://doi.org/10.1093/bioinformatics/btw354 PMID: 27312411; PubMed Central PMCID: PMC5039924.

38. Li H, Durbin R. Fast and accurate short read alignment with Burrows-Wheeler transform. Bioinformatics. 2009; 25(14):1754–60. Epub 20090518. https://doi.org/10.1093/bioinformatics/btp324 PMID: 19451168; PubMed Central PMCID: PMC2705234.

39. Li H, Durbin R. Fast and accurate long-read alignment with Burrows-Wheeler transform. Bioinformatics. 2010; 26(5):589–95. Epub 20100115. https://doi.org/10.1093/bioinformatics/btp698 PMID: 20080505; PubMed Central PMCID: PMC2828108.

40. Li H, Handsaker B, Wysoker A, Fennell T, Ruan J, Homer N, et al. The Sequence Alignment/Map format and SAMtools. Bioinformatics. 2009; 25(16):2078–9. Epub 20090608. https://doi.org/10.1093/bioinformatics/btp352 PMID: 19505943; PubMed Central PMCID: PMC2723002.

41. Liao Y, Smyth GK, Shi W. featureCounts: an efficient general purpose program for assigning sequence reads to genomic features. Bioinformatics. 2014; 30(7):923–30. Epub 20131113. https://doi.org/10.1093/bioinformatics/btt656 PMID: 24227677.

42. Love MI, Huber W, Anders S. Moderated estimation of fold change and dispersion for RNA-seq data with DESeq2. Genome Biol. 2014; 15(12):550. https://doi.org/10.1186/s13059-014-0550-8 PMID: 25516281; PubMed Central PMCID: PMC4302049.

43. Renesh B. reneshbedre/bioinfokit: Bioinformatics data analysis and visualization toolkit. Zenodo; 2020.